High Load-Induced Birefringence of PMMA Investigated in VIS/NIR Spectral Range

Norbert TARJANYI [1], *Milan UHRICIK* [2], *Daniel KACIK* [1], *Peter PALCEK* [2]

[1]Department of Physics, Faculty of Electrical Engineering and Information Technology, University of Zilina, Univerzitna 1, 010 26 Zilina, Slovak Republic
[2]Department of Materials Engineering, Faculty of Mechanical Engineering, University of Zilina, Univerzitna 1, 010 26 Zilina, Slovak Republic

tarjanyi@fyzika.uniza.sk, milan.uhricik@fstroj.uniza.sk, kacik@fel.uniza.sk, peter.palcek@fstroj.uniza.sk

DOI: 10.15598/aeee.v17i3.3449

Abstract. *In the paper, we present the results of an investigation of polymethylmetacrylate's birefringence induced due to applying high-load. The stress-induced birefringence of the polymethylmetacrylate samples was experimentally investigated by an apparatus combining an in-house made plane polariscope with a machine for fatigue testing of materials. A halogen lamp was used as the source of white light. The polariscope's basis was formed by two sets of plane polarizers, one designed for visible (470–750) nm and another one for near-infrared (900–1800) nm spectral range, respectively. The investigated sample was placed between the polarizers and light that passed through the polariscope was collected by an optical fiber connected to an appropriate optical spectral analyzer. The spectra of transmitted light were measured as a function of load and their analysis provided information on the load-induced birefringence of the investigated polymethylmetacrylate samples.*

Keywords

Birefringence, photoelasticity, Polymethylmetacrylate.

1. Introduction

Polymethylmetacrylate (PMMA) is a versatile plastic material used for a wide range of applications in different fields. Due to its transparency and clear nature, it is often used as a glass substitute, e.g. in construction sector in roofing and waterproofing applications, for light pipes and light guides to spread light in the room or as aircraft windows. Due to low cost, volume production, considerable weight reduction and high refractive index and its high variation [1], it is often used for production of lenses [1], [2] and [3], optical fibers, waveguides and optical communication devices [4], optical fibers with Bragg gratings [5], polymer fiber lasers [6] and photonic structures for sensors and display applications [7] and [8]. PMMA based optical components are used in biomedicine thanks to its good biocompatibility, though PMMA is not bioresorbable and such materials are yet to be developed [9] and [10].

PMMA is known for its birefringence occurring due to the process of fabrication [11] or when mechanically manipulated [12]. In many cases, the birefringence is undesired and has to be avoided during fabrication [13] or minimized afterwards. However, if birefringence of material is well defined, the specimen may become very interesting for applications [14]. We investigated the influence of low loads on the strength of the observed photoelastic birefringence of PMMA in Visible (VIS) spectral range [15] and showed the potential of the effect for sensor applications. Here, we present the results of photoelastic birefringence investigation extended also to Near-Infrared (NIR) spectral range and high loads up to 20 kN.

2. Theory

When a monochromatic light wave enters a non-absorbing birefringent medium, it splits into two eigenwaves with mutually orthogonal linear polarizations. The waves possess different refractive indices, i.e. they propagate with different velocities within the medium. After traveling a distance l inside the medium, the phase shift ϕ between the waves emerges. The phase shift ϕ depends on the distance l, the waves' wavelength λ and the difference between light waves' refractive indices, i.e. the birefringence Δn according to:

$$\phi = \frac{2\pi}{\lambda} \cdot l \cdot \Delta n. \quad (1)$$

At the end of the medium, the eigenwaves recombine, and the polarization state of the wave emerging from the medium is defined by the phase shift ϕ between the eigenwaves. Thus, the polarization state of the wave depends on the birefringence of the medium and can be determined using a set of polarization-dependent elements, such as quarter- and half-waveplates, nicol prisms and/or other kinds of polarizers.

In practice, the birefringence of a material can be simply analysed using two plane polarizers and an unpolarized light source. Setting the plane polarizers with mutually perpendicular planes of polarizations to form a centred optical system illuminated by a proper light source one gets an apparatus called plane polariscope. When a birefringent medium is placed in between the polarizers and illuminated (Fig. 1), the intensity I of light at the output of the polariscope can be expressed [16]:

$$I = I_0 \cdot \left[\sin\left(\frac{\phi}{2}\right)\right]^2, \quad (2)$$

where I_0 is the intensity of light impinging the birefringent medium. According to Eq. (1) and Eq. (2) it is clear that the intensity I will vary with wavelength λ of light, thickness l and birefringence Δn of the medium.

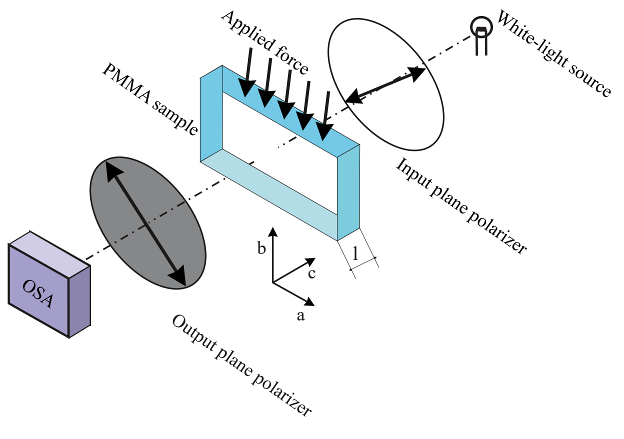

Fig. 1: Apparatus for investigation of birefringence of a medium. Arrows drawn inside the polarizers show the orientation of the planes of polarization. OSA - Optical Spectrum Analyzer.

When a medium placed inside the polariscope shows photoelastic properties its birefringence will vary with force applied perpendicularly to the direction of light propagation (Fig. 1) due to stress-optic law:

$$\Delta n = \Delta n_0 + C \cdot \Delta\sigma. \quad (3)$$

In Eq. (3) Δn_0 represents the birefringence of the medium without applied force, C is the so-called relative stress-optic coefficient, and $\Delta\sigma$ denotes the difference between principal stresses generated in plane perpendicular to the direction of propagation of light due to acting forces.

If a polychromatic source of light is used, for every load applied, one will observe a unique spectral distribution of intensity of light behind the output plane polarizer. Analysis of these spectra provides information on the strength of the induced birefringence.

3. Experiment and Data Evaluation

Investigation of the load-induced birefringence was performed on commercially available plates of PMMA. They were cut to form blocks with dimensions ($a \times b \times c$) equal (82.95 × 19.924 × 9.572) mm^3. The samples were made of clear PMMA plates with "c" planes being transparent. The thickness l of the samples was 9.572 mm. The dimensions along "b-" and "c-" directions were measured with an error ±0.005 mm and the dimension along "a-" direction was measured with an error equal to ±0.05 mm.

The polariscope was built using a halogen lamp-based white-light source SLS201/M (by Thorlabs) and two sets of plane polarizers. The used sets of VIS and NIR polarizers were designed for wavelength range (470–750) nm and (900–1800) nm, respectively. Light that passed through the polariscope was collected by an optical fiber with 400 µm core diameter and numerical aperture equal 0.39. The fiber was connected to optical spectral analyzer HR2000$^+$ (by Ocean Optics) with resolution 0.5 nm for measurements in VIS spectral region and to NIRQuest 512 (by Ocean Optics) with resolution 4 nm when performing the measurements in NIR spectral region.

In order to investigate the load-induced birefringence of PMMA samples, we combined the polariscope with a machine for fatigue testing of materials and/or components Vibrophore Amsler 150 HFP 5100 (Zwick/Roell). All measurements were done at room temperature.

3.1. Estimation of Residual Birefringence

PMMA belongs to a class of polymers that exhibit birefringence due to the fabrication process and/or mechanical manipulation like cutting or forming (usually at temperatures higher than 20 degrees Celsius) [11], [14], [17] and [18]. This kind of birefringence exists in the PMMA sample as a remnant after its processing history, so it is often named as residual one. For the purpose of further investigation, we will denote the residual birefringence Δn_0 (see Eq. (3)).

In order to find the residual birefringence, we put a sample on a rotary stage placed in between the crossed polarizers, rotated the sample in a vertical plane from 0 degrees to 360 degrees with 5 degree steps and recorded the spectrum observed at the output of the polariscope for every angle of rotation. The procedure was done twice: once when VIS and the second when NIR polarizers were used. The recorded spectra for angles from 0 degrees to 45 degrees with respect to the initial position are plotted in Fig. 2.

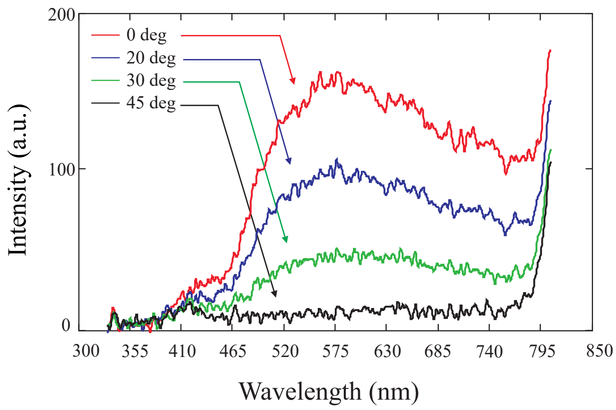

(a) VIS spectral range.

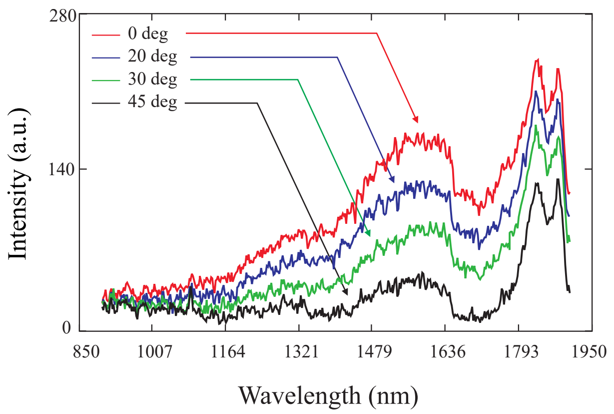

(b) NIR spectral range.

Fig. 2: Spectra of light transmitted through the polariscope with inserted sample of PMMA for various angles of rotation obtained in VIS and NIR spectral ranges.

The sets of spectra obtained in VIS and NIR spectral ranges as a function of angle of rotation were normalized and used for estimation of the residual birefringence. According to Eq. (1), for birefringent sample with constant thickness l and without load, the phase shift ϕ will only depend on the wavelength λ and the residual birefringence Δn_0. The value of Δn_0 as a function of wavelength was obtained by fitting the normalized intensity of light (from Eq. (2) and using Eq. (1)) to the measured data expressed as a function of the rotation angle [12].

For illustration, in Fig. 3, there is shown the result of the fitting procedure performed for data measured at wavelength 532 nm. Due to rather low residual birefringence of the investigated PMMA samples, the magnitudes of the measured spectra were also rather low, so the influence of the noise was not negligible. This is reflected in some variation of the measured data (see Fig. 2). Nevertheless, the fitting process runs successfully (see Fig. 3), and the best fit gave the value of Δn_0 being $-1.99 \cdot 10^{-5}$ for wavelength 532 nm. The value of $\Delta n_0 < 0$ was accepted as it is known that the birefringence of PMMA is negative [14] and [17]. Applying the fitting procedure on every measured spectrum in VIS and NIR spectral ranges, we obtained the wavelength dependence of the residual birefringence Δn_0 of the investigated PMMA sample.

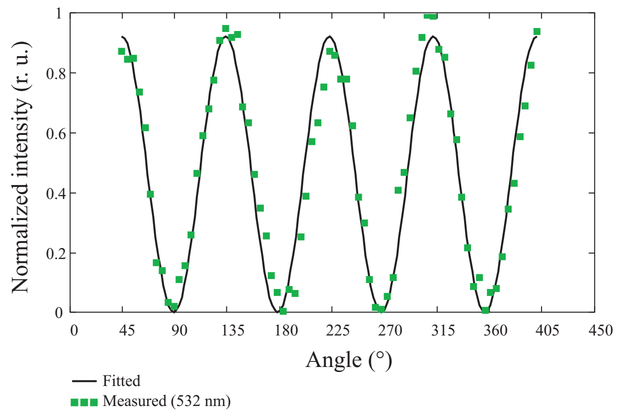

Fig. 3: Measured and calculated normalized intensity as function of rotation angle for wavelength $\lambda = 532$ nm.

In order to minimize the influence of the noise, the obtained dependence was smoothed and the result is shown in Fig. 4. These smoothed dependences were used for evaluation of measured data obtained when performing an investigation of the effect of the load on PMMA's birefringence.

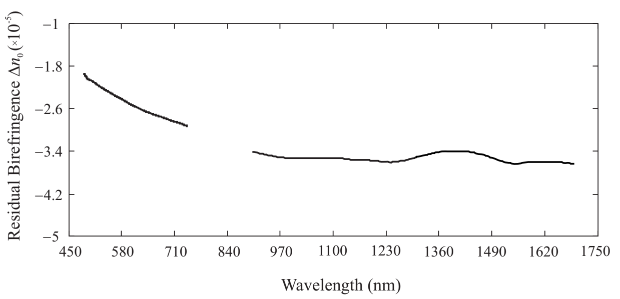

Fig. 4: Estimated wavelength dependence of the residual birefringence Δn_0 of the investigated PMMA sample.

3.2. Load-Induced Birefringence

In order to investigate the influence of the external forces on the birefringence of PMMA samples, we integrated the polariscope with a machine for fatigue testing of materials Vibrophore Amsler 150 HFP 5100. First, the increasing load was applied to a test sample as illustrated in Fig. 1 in order to estimate the range of loads for which the PMMA exhibits elastic deformation. The force was gradually applied on the upper side of the sample, and the displacement of the Vibrophore's loading head from its initial position was measured at the same time. The displacement was measured using a gauge Imeko EDK 93 with accuracy 0.01 µm and a total travel distance of the probe being 1 mm.

According to our previous measurements done on smaller samples [15], we estimated the upper limit for actually used bigger samples to be about 20,000 N. After reaching 20,100 N the sample was gradually unloaded while the displacement of the loading head was still measured. During the whole test, the sample was placed in the polariscope and spectrum at the output was recorded in order to control the physical contact between the sample and the loading head. The measurement of the loading head's displacement showed that the dimension of the sample did not change after its unloading. This was also proved by comparing those spectra recorded before and after the sample's loading as there was not observed any difference between them.

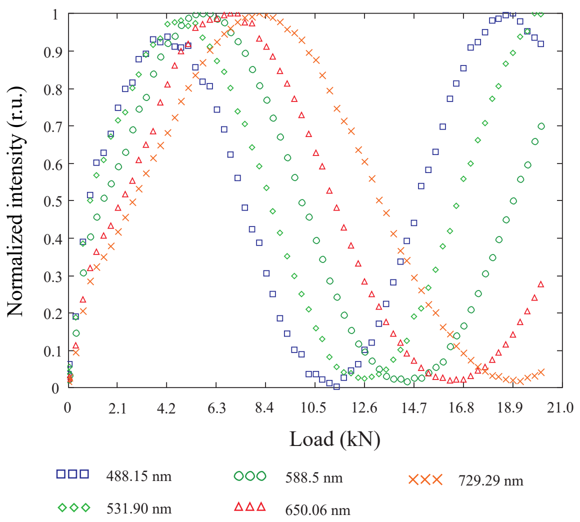

(a) VIS spectral range.

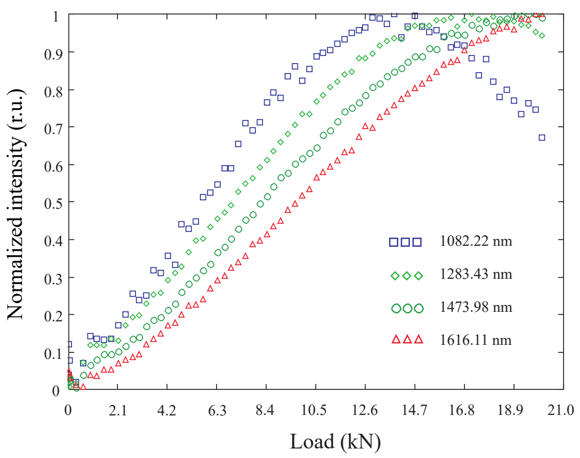

(b) NIR spectral range.

Fig. 5: Normalized intensities of light at the output of the polariscope for selected wavelengths in VIS and NIR spectral ranges as function of the applied load.

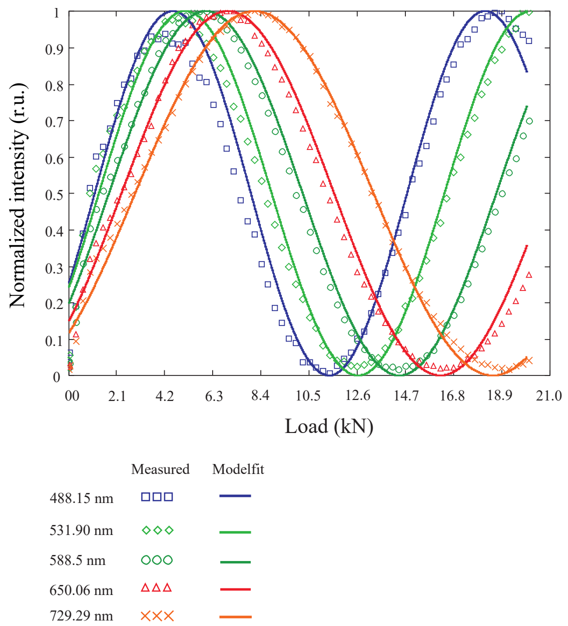

(a) VIS spectral range.

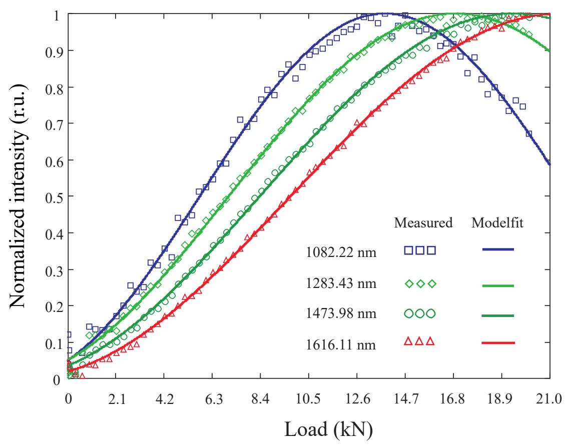

(b) NIR spectral range.

Fig. 6: Normalized intensity of light at the output of the polariscope for selected wavelengths in VIS and NIR spectral ranges as function of the applied load fitted by normalized intensity calculated according to Eq. (4).

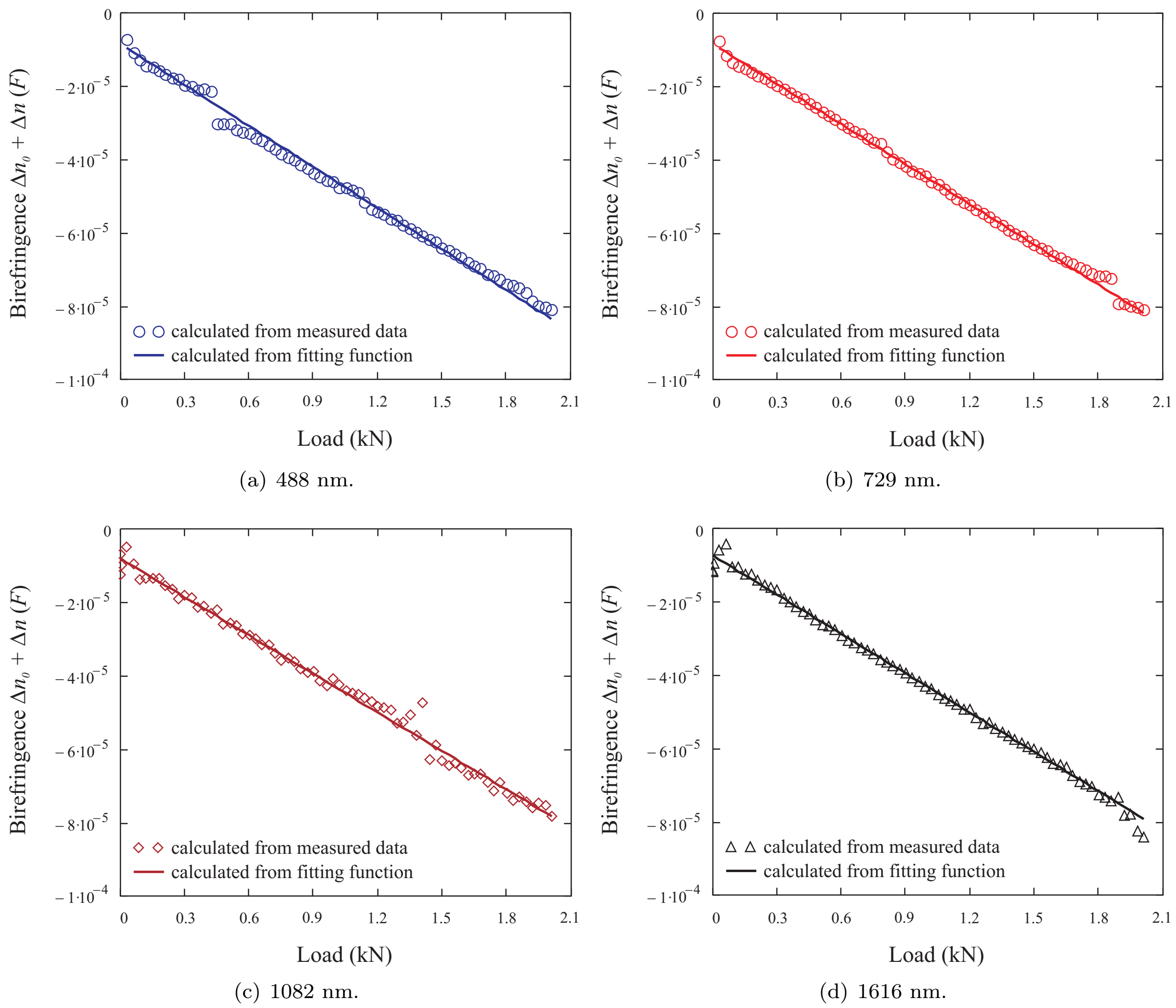

(a) 488 nm.

(b) 729 nm.

(c) 1082 nm.

(d) 1616 nm.

Fig. 7: Total birefringence as function of the load plotted for wavelengths 488 nm, 729 nm, 1082 nm and 1616 nm.

After experimental determination of the range of loads causing the elastic deformation, we repeated deforming the samples in order to examine the load-induced birefringence. The curves plotted in Fig. 5 represent the normalized intensities of transmitted light of selected wavelengths in VIS and NIR spectral regions as a function of the load.

The dependences plotted in Fig. 5 clearly show the effect of the applied load on the birefringence of PMMA. The load-induced birefringence can be quantified using Eq. (1), Eq. (2) and Eq. (3) and measured dependences. Putting Eq. (3) into Eq. (1) and its subsequent substitution in Eq. (2) leads to an expression for the intensity of light observed behind the polariscope as a function of the applied load:

$$I = I_0 \cdot \left\{ \sin \left[\frac{\pi \cdot l}{\lambda} \cdot \left(\Delta n_0 + C \cdot \frac{F}{S} \right) \right] \right\}^2. \quad (4)$$

In Eq. (4), the ratio $\frac{F}{S}$ expresses the difference between principal stresses $\Delta\sigma$ from Eq. (3), where F is the applied load and S is the area of the loaded side of the sample.

Equation (4) now represents a model which can be used for fitting the measured data, thus providing the dependence of the birefringence of the PMMA sample on the applied load. The result of the fitting process for selected wavelengths in VIS and NIR spectral ranges is shown in Fig. 6. In Eq. (4), we used values of the obtained residual birefringence Δn_0 while values of the coefficient C were subject to fitting. However, the best match between measured and calculated dependences was achieved by fitting not only the coefficient C but also the residual birefringence Δn_0.

The comparison between values of residual birefringence Δn_0 obtained by independent measurement performed in a way mentioned in Sec. 3.1. and those obtained due to the fitting of the measured data by the dependence expressed by Eq. (4) showed some differences. Nevertheless, both sets of the obtained dependences Δn_0 fall within the same order of magnitude. The slight discrepancy can be attributed to noise observed in the measured spectra (see Fig. 2) and subsequent smoothing of the data representing the estimated residual birefringence (see Fig. 4).

The result of fitting the normalized intensity of light derived from Eq. (4) to the normalized intensity of light measured as a function of the load is the dependence of birefringence on the load $\Delta n(F)$. The dependence can be compared with that obtained from the measured and normalized data. The total birefringence (residual and load-induced) as a function of the load is for selected wavelengths plotted in Fig. 7.

For illustration, data for wavelengths at the beginning and the end of the investigated VIS and NIR spectral ranges were chosen for plotting. Figure 7 shows a very good match between birefringence calculated from the measured normalized data and those calculated from the function $\Delta n(F)$ obtained by the fitting.

It is clear that the load-induced birefringence of PMMA follows the linear stress optic law also for rather high loads up to 20 kN. This property of PMMA is promising and can be used for the construction of various kinds of load sensors.

4. Conclusion

We investigated the birefringence of PMMA samples due to applied load. For the investigation, we used plane polariscope employing two independent sets of plane polarizers, one designed for VIS and the other one for NIR spectral regions. The polariscope was integrated with the machine for fatigue testing of materials Vibrophore Amsler 150 HFP 5100 (Zwick/Roell) used for deformation of the PMMA samples. The dependences of the spectral distribution of intensity of light on the load applied to the samples of PMMA placed in the plane polariscope measured at the output of the polariscope were used for determination of load-induced birefringence. It was shown that the load-induced birefringence of PMMA follows the linear stress optic law also for rather high loads up to 20 kN. This linear dependence of the birefringence on the load allows using PMMA for construction of physical elements of various kinds of load sensors such as a sensor of weight, force or normal pressure.

Acknowledgment

This work was supported by Slovak Research and Development Agency under the project No. APVV-15-0441.

References

[1] YANG, C., L. SU, C. HUANG, H.-X. HUANG, J. M. CASTRO and A. Y. YI. Effect of packing pressure on refractive index variation in injection molding of precision plastic optical lens. *Advances in Polymer Technology*. 2011, vol. 30, iss. 1, pp. 51–61. ISSN 0730-6679. DOI: 10.1002/adv.20211.

[2] JIN, Y., H. TAI, A. HILTNER, E. BAER and J. S. SHIRK. New class of bioinspired lenses with a gradient refractive index. *Journal of Applied Polymer Science*. 2007, vol. 103, iss. 3, pp. 1834–1841. ISSN 1097-4628. DOI: 10.1002/app.25404.

[3] LANGUY, F., K. FLEURY, C. LENAERTS, J. LOICQ, D. REGAERT, T. THIBERT and S. HABRAKEN. Flat Fresnel doublets made of PMMA and PC: combining low cost production and very high concentration ratio for CPV. *Optics Express*. 2011, vol. 19, iss. S3, pp. A280–A294. ISSN 1094-4087. DOI: 10.1364/OE.19.00A280.

[4] BLYTHE, A. R. and J. R. VINSON. Polymeric materials for devices in optical fibre systems. *Polymers for Advanced Technologies*. 2000, vol. 11, iss. 8, pp. 601–611. ISSN 1099-1581. DOI: 10.1002/1099-1581(200008/12)11:8/12<601::AID-PAT10>3.0.CO;2-%23.

[5] YUAN, W., A. STEFANI, M. BACHE, T. JACOBSEN, B. ROSE, N. HERHOLDT-RASMUSSEN, F. K. NIELSEN, S. ANDERSEN, O. B. SORENSEN, K. S. HANSEN and O. BANG. Improved thermal and strain performance of annealed polymer optical fiber Bragg gratings. *Optics Communications*. 2011, vol. 284, iss. 1, pp. 176–182. ISSN 0030-4018. DOI: 10.1016/j.optcom.2010.08.069.

[6] CASPARY, R., F. JAKOBS, J. KIELHORN, P. Y. ANG, M. CEHOVSKI, M. BECK, H.-H. JOHANNES, S. BALENDAT, J. NEUMAN, S. UNLAND, S. SPELTHANN, J. THIEM, A. RUEHL, D. RISTAU and W. KOWALSKY. Polymer fiber lasers. In: *21st Internation Conference On Transparent Optical Networks (ICTON)*. Angers: 2019. pp. 1–4. ISBN 978-1-7281-2779-8. DOI: 10.1109/ICTON.2019.8840399.

[7] POTYRAILO, R. A. Sensors in combinatorial polymer research. *Macromolecular rapid communications*. 2004, vol. 25, iss. 1, pp. 77–94. ISSN 1022-1336. DOI: 10.1002/marc.200300212.

[8] LEE, J.-H., C. Y. KOH, J. P. SINGER, S.-J. JEON, M. MALDOVAN, O. STEIN and

E. L. THOMAS. 25th anniversary article: Ordered polymer structures for the engineering of photons and phonons. *Advanced Materials*. 2014, vol. 26, iss. 4, pp. 532–569. ISSN 0935-9648. DOI: 10.1002/adma.201303456.

[9] PODRAZKY, O., P. PETERKA, I. KASIK, S. VYTYKACOVA, J. PROBOSTOVA, J. MRAZEK, M. KUNES, V. ZAVALOVA, V. RADOCHOVA, O. LYUTAKOV, E. CECI-GINISTRELLI, D. PUGLIESE, N. G. BOETTI, D. JANNER and D. MILANESE. In vivo testing of a bioresorbable phosphate-based optical fiber. *Journal of Biophotonics*. 2019, vol. 12, iss. 7, pp. 1–6. ISSN 1864-0648. DOI: 10.1002/jbio.201800397.

[10] GIEREJ, A., M. VAGENENDE, A. FILIPKOWSKI, B. SIWICKI, R. BUCZYNSKI, H. THIENPONT, S. VAN VLIERBERGHE, T. GEERNAERT, P. DUBRUEL and F. BERGHMANS. Poly (D, L-lactic acid)(PDLLA) biodegradable and biocompatible polymer optical fiber. *Journal of Lightwave Technology*. 2019, vol. 37, iss. 9, pp. 1916–1923. ISSN 1558-2213. DOI: 10.1109/JLT.2019.2895220.

[11] KOJO, T., A. TAGAYA and Y. KOIKE. Mechanism of generation of birefringence in poly (methyl methacrylate/styrene). *Polymer Journal*. 2012, vol. 44, iss. 1, pp. 167–173. ISSN 1349-0540. DOI: 10.1038/pj.2011.101.

[12] REDNER, A. S. and B. HOFFMAN. Residual stress testing for transparent polymers. In: *Strainoptics* [online]. 1999. Available at: `http://www.strainoptics.com/wp-content/uploads/2017/07/Residual-Stress-Testing.pdf`.

[13] TAHAYA, A. and Y. KOIKE. Compensation and control of the birefringence of polymers for photonics. *Polymer Journal*. 2012, vol. 44, iss. 1, pp. 306–314. ISSN 1349-0540. DOI: 10.1038/pj.2011.141.

[14] LORKOWSKI, H.-J., K. PFEIFFER, M. BIEBRICHER and H. FRANKE. Optical polymers with special birefringent properties. *Polymers for Advanced Technologies*. 1996, vol. 7, iss. 5, pp. 501–506. ISSN 1042-714. DOI: 10.1002/(SICI)1099-1581(199605)7:5/6<501::AID-PAT537>3.0.CO;2-M.

[15] TARJANYI, N., D. KACIK, M. UHRICIK and P. PALCEK. Investigation of birefringence of elastically deformed poly (methyl methacrylate). In: *2018 ELEKTRO*. Mikulov: IEEE, 2018, pp. 1–5. ISBN 978-1-5386-4759-2. DOI: 10.1109/ELEKTRO.2018.8398340.

[16] BORN, M. and E. WOLF. *Principles of optics: electromagnetic theory of propagation, interference and diffraction of light*. 7th. ed. Cambridge: Cambridge University Press, 2003. ISBN 978-052-1642-224.

[17] SHAFIEE, H., A. TAGAYA and Y. KOIKE. Mechanism of generation of photoelastic birefringence in methacrylate polymers for optical devices. *Journal of Polymer Science Part B: Polymer Physics*. 2010, vol. 48, iss. 19, pp. 2029–2037. ISSN 0887-6266. DOI: 10.1002/polb.22082.

[18] SHAFIEE, H., S. BEPPU, S. IWASAKI, A. TAGAYA and Y. KOIKE. Mechanisms of orientational and photoelastic birefringence generation of methacrylates for the design of zero-zero-birefringence polymers. *Polymer Engineering & Science*. 2015, vol. 55, iss. 6, pp. 1330–1338. ISSN 0032-3888. DOI: 10.1002/pen.24072.

About Authors

Norbert TARJANYI was born in Presov, Slovak Republic. He is an Associate Professor at the Department of Physics, University of Zilina, Slovak Republic. His research interests include photoelasticity of polymers, birefringence of polymers and crystals, light-matter interaction and sensors.

Milan UHRICIK was born in Dolny Kubin, Slovak Republic. He received his M.Sc. from University of Zilina in Applied Mechanics in 2010. His research interests include applied mechanics, low-frequency fatigue of materials, realization of cyclic loading, measurement of internal damping, modeling of load and deformation around fatigue crack and measurement of fatigue increment per load cycle.

Daniel KACIK was born in Topolcany, Slovak Republic. He received his M.Sc. and Ph.D. from University of Zilina in Telecommunications in 2000 and 2004, respectively. His research interests include interferometry and specialty optical fibers-based sensors.

Peter PALCEK was born in Koseca, Slovak Republic. He is Professor in Material Engineering. His research interests include relationship between structure and material properties, scanning electron microscopy and internal material dumping.